Research Article | Vol. 25, No. 16 | 7 Aug 2017 | OPTICS EXPRESS A798
Optics EXPRESS

Impact of spectral resolution of *in situ* ocean color radiometric data in satellite matchups analyses

GIUSEPPE ZIBORDI,[1,*] MARCO TALONE,[1] KENNETH J. VOSS,[2] AND B. CAROL JOHNSON[3]

[1]*European Commission, Joint Research Centre, 21027 Ispra, Italy*
[2]*University of Miami, Coral Gables, Florida 33124, USA*
[3]*Sensor Science Division, National Institute of Standards and Technology, Gaithersburg, MD, USA*
[*]*giuseppe.zibordi@ec.europa.eu*

Abstract: The spectral resolution requirements for *in situ* remote sensing reflectance R_{RS} measurements aiming at supporting satellite ocean color validation and System Vicarious Calibration (SVC) were investigated. The study, conducted using sample hyperspectral R_{RS} from different water types, focused on the visible spectral bands of the Ocean Land Color Imager (OLCI) and of the Plankton, Aerosol, Cloud, ocean Ecosystem (PACE) satellite sensors. Allowing for a ±0.5% maximum difference between *in situ* and satellite derived R_{RS} solely due to the spectral band characteristics of the *in situ* radiometer, a spectral resolution of 1 nm for SVC of PACE is needed in oligotrophic waters. Requirements decrease to 3 nm for SVC of OLCI. In the case of validation activities, which exhibit less stringent uncertainty requirements with respect to SVC, a maximum difference of ±1% between *in situ* and satellite derived data indicates the need for a spectral resolution of 3 nm for both OLCI and PACE in oligotrophic waters. Conversely, spectral resolutions of 6 nm for PACE and 9 nm for OLCI appear to satisfy validation activities in optically complex waters.

OCIS codes: (280.0280) Remote sensing and sensors; (120.0120) Instrumentation, measurement, and metrology.

References and links

1. World Meteorological Organization (WMO), *The Global Observing System for Climate: Implementation needs*. Report GCOS – 200 (2016) (available at *http://unfccc.int/files/science/workstreams/systematic_observation/application/pdf/gcos_ip_10oct2016.pdf*).
2. H. R. Gordon, "Calibration requirements and methodology for remote sensors viewing the ocean in the visible," Remote Sens. Environ. **22**(1), 103–126 (1987).
3. G. Zibordi, J.-F. Berthon, F. Mélin, D. D'Alimonte, and S. Kaitala, "Validation of satellite ocean color primary products at optically complex coastal sites: Northern Adriatic Sea, Northern Baltic Proper and Gulf of Finland," Remote Sens. Environ. **113**(12), 2574–2591 (2009).
4. F. Mélin and G. Sclep, "Band shifting for ocean color multi-spectral reflectance data," Opt. Express **23**(3), 2262–2279 (2015).
5. M. R. Wernand, S. J. Shimwell, and J. C. De Munck, "A simple method of full spectrum reconstruction by a five-band approach for ocean colour applications," Int. J. Remote Sens. **18**(9), 1977–1986 (1997).
6. Z. Lee, S. Shang, C. Hu, and G. Zibordi, "Spectral interdependence of remote-sensing reflectance and its implications on the design of ocean color satellite sensors," Appl. Opt. **53**(15), 3301–3310 (2014).
7. B. C. Johnson, S. Flora, S. Brown, D. Clark, M. Yarbrough, and K. Voss, "Spectral resolution requirements for vicarious calibration of ocean color satellites". Presented at the Ocean Color Research Team Meeting, Seattle (2007), available at *http://oceancolor.gsfc.nasa.gov/cms/DOCS/ScienceTeam/OCRT_Apr2007/Posters/*.
8. D. K. Clark, H. R. Gordon, K. J. Voss, Y. Ge, W. Broenkow, and C. Trees, "Validation of atmospheric correction over the oceans," J. Geophys. Res. **102**(17), 209–217 (1997).
9. S. W. Brown, S. J. Flora, M. E. Feinholz, M. A. Yarbrough, T. Houlihan, D. Peters, K. Y. S. Kim, J. L. Mueller, B. C. Johnson, and D. K. Clark, "The Marine Optical BuoY (MOBY) radiometric calibration and uncertainty budget for ocean color satellite sensor vicarious calibration," in SPIE Conference Proceedings *Remote Sensing,* pp. 67441M–67441M. International Society for Optics and Photonics (2007).
10. G. Zibordi, J.-F. Berthon, F. Mélin, and D. D'Alimonte, "Cross-site consistent in situ measurements for satellite ocean color applications: The BiOMaP radiometric dataset," Remote Sens. Environ. **115**(8), 2104–2115 (2011).
11. A. Tonizzo, M. Twardowski, S. McLean, K. Voss, M. Lewis, and C. Trees, "C. and Trees, "Closure and uncertainty assessment for ocean color reflectance using measured volume scattering functions and reflective tube absorption coefficients with novel correction for scattering," Appl. Opt. **56**(1), 130–146 (2017).

#290731 https://doi.org/10.1364/OE.25.00A798
Journal © 2017 Received 15 Mar 2017; revised 29 May 2017; accepted 30 May 2017; published 21 Jul 2017

Optics EXPRESS

12. M. Berger, J. Moreno, J. A. Johannessen, P. F. Levelt, and R. F. Hanssen, "ESA's sentinel missions in support of Earth system science," Remote Sens. Environ. **120**, 84–90 (2012).
13. C. Del Castillo, *Pre-Aerosol, Clouds, and ocean Ecosystem (PACE) Mission science definition team report* (2012), *available at https://pace.oceansciences.org/docs/pace_sdt_report_final.pdf.*
14. B. A. Franz, S. W. Bailey, P. J. Werdell, and C. R. McClain, "Sensor-independent approach to the vicarious calibration of satellite ocean color radiometry," Appl. Opt. **46**(22), 5068–5082 (2007).
15. S. W. Bailey, S. B. Hooker, D. Antoine, B. A. Franz, and P. J. Werdell, "Sources and assumptions for the vicarious calibration of ocean color satellite observations," Appl. Opt. **47**(12), 2035–2045 (2008).
16. G. Zibordi, F. Mélin, K. J. Voss, B. C. Johnson, B. A. Franz, E. Kwiatkowska, J.-P. Huot, M. Wang, and D. Antoine, "System vicarious calibration for ocean color climate change applications: Requirements for *in situ* data," Remote Sens. Environ. **159**, 361–369 (2015).

1. Introduction

Satellite ocean color radiometric products, such as the water-leaving radiance, L_W, or the related remote sensing-reflectance, R_{RS}, are the fundamental quantities used to generate geo-physical data products (e.g., chlorophyll concentration, *Chla*). Accuracy requirements set for these derived products [1,2] bound uncertainty requirements for satellite radiometric data.

Presently, post-launch system vicarious calibration (SVC) [2] is the only viable approach allowing satellite radiometric data to meet the level of uncertainty that satisfies requirements for ocean color products. The SVC process implies the use of highly accurate *in situ* radiometric measurements. *In situ* radiometric data are also frequently applied to investigate uncertainties affecting satellite products through validation exercises.

Markedly, both validation and SVC applications rely on matchups (i.e., time and space coincident) of *in situ* and satellite ocean color radiometric data. This implies a comprehensive assessment of the various sources of uncertainty affecting the *in situ* measurements, which include radiometric, methodological and environmental factors. A source of uncertainty, which causes systematic differences between *in situ* and satellite radiometric data, but is controllable by instrument design, is the diversity of spectral characteristics of *in situ* and satellite ocean color sensors due to the different widths, shapes and center-wavelengths of corresponding spectral bands. This uncertainty can be minimized through the application of corrections (i.e., band-shifting) obtained by modeling the spectral dependence of radiometric quantities such as R_{RS} [3,4]. This solution, however, may still be subject to substantial uncertainties due to the lack of accurate information on seawater optical properties and additionally by incomplete information on the spectral response functions of *in situ* sensors. An alternative solution is given by the statistical reconstruction of R_{RS} from discrete values measured in various spectral bands [5,6]. In this case, the uncertainties affecting the determination of R_{RS} spectra depend on the number of spectral bands, their location and width. As the portion of the uncertainties that are driven by environmental factors and the radiometric calibration process, when combined, can be a large fraction of the desired maximum limit, it is critical that those factors that can be controlled by instrument design be minimized and do not add significantly to the combined uncertainty budget for the *in situ* data.

The problem of spectral differences can be reduced with *in situ* hyperspectral data (i.e., data collected with a relatively large number of narrow spectral bands distributed continuously over the spectrum). In fact, compared to multispectral measurements, *in situ* hyperspectral data allow the determination of R_{RS} in the spectral bands of the satellite sensor with an accuracy increasing with the spectral resolution (defined by the sensor bandwidth $\Delta\lambda_B$ determined by the full width at half maximum spectral response) and the spectral sampling interval (i.e., the distance between center-wavelengths of adjacent bands $\Delta\lambda_C$) of the *in situ* sensor.

Thus, hyperspectral *in situ* radiometric data can be the optimum solution for SVC data due to the need to minimize this source of uncertainty in the accurate determination of mission

specific gain-factors (i.e., *g*-factors) for satellite radiometric data. Specifically, as an extreme case, the accessibility of sub-nanometer radiometric spectra would allow accurate R_{RS} values to be determined for any multispectral or hyperspectral space sensor. In fact, assuming the satellite sensor is comprehensively characterized, *in situ* sub-nanometer spectra would allow the satellite spectral response functions and out-of-band or stray light perturbations to be fully accounted for. However, the technological complexity, and cost, intrinsic in sub-nanometer radiometer systems suggests that there may be a tradeoff between spectral resolution and allowable uncertainty.

The overall objective of this work, which expands on a previous assessment [7], is to investigate the impact of the spectral resolution of *in situ* radiometric data on the determination of R_{RS} at bands representative of current and forthcoming ocean color sensors. The analysis aims at estimating the sole contribution of spectral resolution to the uncertainty budget affecting the comparison of *in situ* and satellite R_{RS}. It specifically focuses on the visible spectral bands of the Ocean Land Color Imager (OLCI) from the European Space Agency (ESA) operating onboard Sentinel-3 since 2016, and of the Plankton, Aerosol, Cloud, ocean Ecosystem (PACE) of the National Aeronautics and Space Administration (NASA) planned for launch in 2022.

2. Data and methods

The study relies on sample R_{RS} spectra from marine waters characterized by varying concentrations of optically significant constituents. These spectra are applied to investigate differences between *in situ* and satellite data solely due to dissimilar spectral bands. Recalling that the analysis is restricted to satellite bands representative of current multispectral and future hyperspectral ocean color systems, the final objective of the work is the definition of requirements for *in situ* hyperspectral sensors supporting validation and SVC applications. It is emphasized that the study is focused on the impact of spectral resolution on *in situ* radiometric measurements and excludes any other source of uncertainty that may affect matchup analysis, or correction schemes that may minimize spectral differences between sensors.

2.1 Data

The study is performed using samples of *in situ* hyperspectral radiometric data representative of various water types. The fundamental quantities are the R_{RS} spectra displayed in Fig. 1 and determined from the ratio of water leaving radiance L_W to downward irradiance E_S. One sample R_{RS} spectra was obtained with the Marine Optical System (MOS) from fixed-depth measurements performed in ultra-oligotrophic waters at the Marine Optical Buoy (MOBY) site with spectral resolution $\Delta\lambda_B$ of 1 nm and a spectral sampling interval $\Delta\lambda_C$ of approximately 0.6 nm [8,9]. Additional sample data are R_{RS} spectra from above-water radiometric measurements performed with RAMSES hyperspectral radiometers in various European seas. These embrace oligotrophic waters in the Western Mediterranean Sea, and optically complex waters in the Western Black and northern Adriatic Seas. RAMSES radiometers, manufactured by TriOS (Rastede, Germany), have a spectral resolution of approximately 10 nm and a nominal spectral sampling interval of 3.3 nm. Clearly, while MOS spectra are suitable to address investigations up to approximately 1 nm spectral resolution, RAMSES data may not fully satisfy requirements to assess R_{RS} spectral matching at resolutions lower than several nanometers. The uncertainties associated with this limitation, are addressed in the discussion section. It is however anticipated that, while MOS spectra are mostly applied to address both the validation and highly demanding SVC requirements in oligotrophic

Optics EXPRESS

waters, RAMSES data are only used to draw general conclusions on the less stringent requirements for the validation of satellite products in optically complex waters.

The analysis is restricted to the spectral region between 380 nm and 700 nm for which the considered *in situ* radiometric data exhibit reliable values (i.e., not largely affected by reduced sensitivity of the radiometers or an input signal that is too small), and additionally represent the spectral region of utmost interest for both validation and SVC activities. With respect to this, there are some peculiar features near 400 nm in the spectrum representing ultra-oligotrophic waters as displayed in Fig. 1. These can be explained by slight differences on the order of 0.1 nm in E_S and L_W spectral calibrations in a region characterized by Fraunhofer lines in the solar irradiance. Because of this, results related to such a narrow spectral region need to be considered with some caution.

Details of water bio-optical quantities related to the R_{RS} spectra included in the analysis are summarized in Table 1. These include *Chla*, concentration of total suspended matter, *TSM*, and the absorption coefficient, *a*, and backscattering coefficient, b_b, at 490 nm of optically significant water constituents. Their values fully support the diversity of cases represented by the R_{RS} spectra considered.

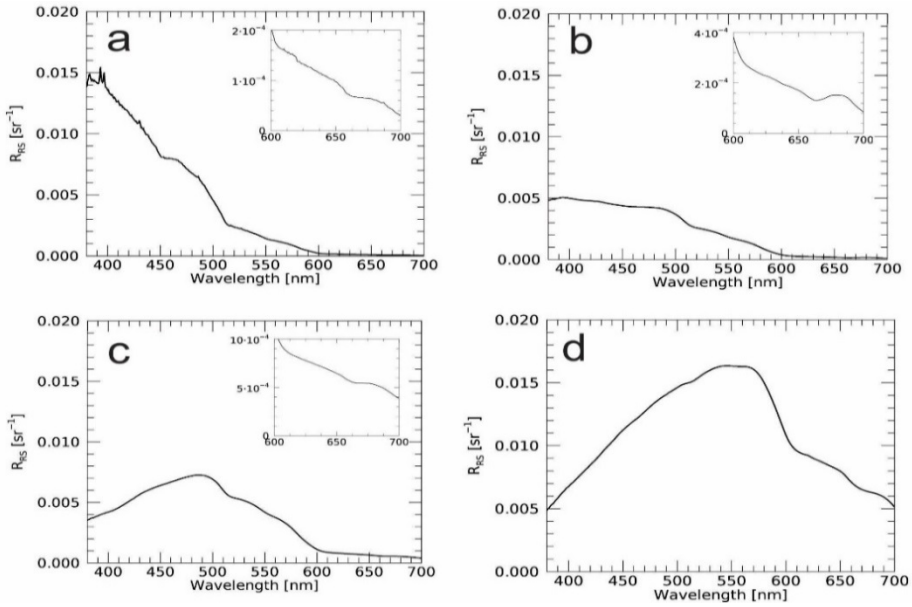

Fig. 1. Sample R_{RS} spectra used in this study. NP (a) and WM (b) refer to the North Pacific Gyre and the Western Mediterranean Sea oligotrophic waters, while WB (c) and NA (d) refer to the Western Black Sea and northern Adriatic optically complex waters. Insets in panels a-c display R_{RS} with scales expanded in the 600-700 nm interval to better visualize spectral features.

Optics EXPRESS

Table 1. Bio-optical quantities(a) related to the R_{RS} spectra used in this study: *Chla* and *TSM* indicate the concentration of chlorophyll-a and of total suspended matter, while *a* and b_b indicate the absorption and backscattering coefficients at 490 nm of optically significant constituents, respectively.

Region	Date [dd/mm/yyyy]	Sun zenith [°]	*Chla* [µg l^{-1}]	*TSM* [mg l^{-1}]	*a*(490) [m^{-1}]	b_b(490) [m^{-1}]
North Pacific Gyre (NP)	15/06/2015	4.1	0.13(b)	0.10(b)	0.019(c)	0.0027(c)
Western Med. Sea (WM)	18/04/2014	29.2	0.35	0.24	0.037	0.0027
Western Black Sea (WB)	05/06/2016	45.2	0.27	0.44	0.048	0.0058
North Adriatic Sea (NA)	08/04/2015	54.3	2.68	6.30	0.149	0.0528

[a]from the BioMAP [10] data set.
[b]provided by Stephanie Flora (Moss Landing Marine Labs);
[c]from published values [11], here increased by the pure seawater contribution.

2.2 Spectral bands of satellite sensors

As already mentioned, this study is centered on OLCI [12], representative of current global satellite ocean color sensors, and additionally on PACE [13], which is assumed to be representative of future advanced hyperspectral earth observing systems. While OLCI relies on spectral bands commonly exhibiting 10 nm bandwidth in the visible spectral region (15 nm at 400 nm), PACE will have a large number of bands with 5 nm bandwidth from the ultraviolet to the near-infrared. Consequently, PACE-like bands have been designed by assuming 5 nm bandwidth, an ideal Gaussian spectral response function, and 5 nm spectral sampling interval. It is recognized that this solution produces a sampling of R_{RS} spectra that may differ slightly from actual capabilities of the future space sensor.

The relative spectral response functions for OLCI and PACE-like bands are illustrated in Fig. 2.

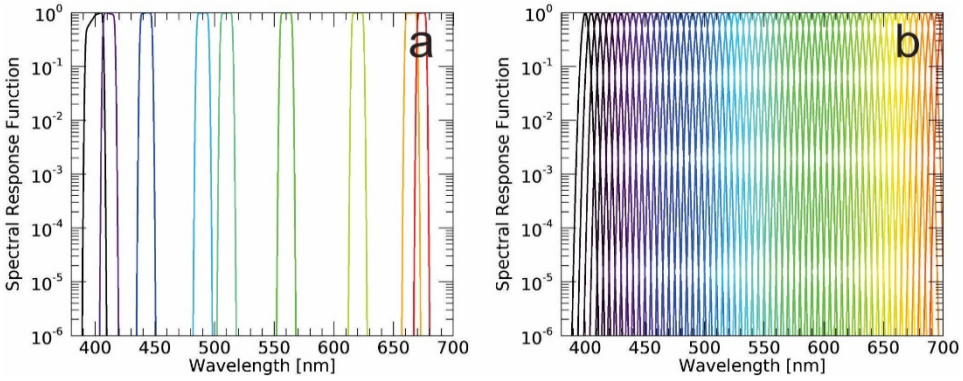

Fig. 2. Relative spectral response functions of the visible OLCI (a) and PACE-like (b) bands.

2.3 Band spectral matching

The spectral matching scheme introduced in this section has been devised to investigate differences between R_{RS} obtained with OLCI or PACE-like sensors, and R_{RS} values

reconstructed with *in situ* hyperspectral data having various spectral resolutions and sampling intervals. These differences introduce uncertainties in the SVC process, and are also relevant for the application of *in situ* data to the validation of satellite radiometric products requiring the comparison of satellite and *in situ* R_{RS} values.

It is emphasized that regardless of the focus on R_{RS}, L_W and E_S are processed separately before computing R_{RS} (i.e., $R_{RS} = L_W / E_S$) to fully account for the independence of L_W and E_S measurements from different radiometers.

The flow diagram in Fig. 3 summarizes the matching scheme. The different radiometric quantities identified in the diagram and applied in the following analysis (i.e., L_W, E_S or R_{RS}) are hereafter indicated using the generic variable $\Re$. Specifically,

$\Re^n$: sample L_W and E_S values from MOS or RAMSES hyperspectral sensors;

$\Re^r$: reference L_W and E_S hyperspectral values determined from the resampling at higher spectral resolution (i.e., 0.1 nm) through linear interpolation of the $\Re^n$ sample spectra;

$\Re^s$: satellite-exact radiometric values determined from $\Re^r$ accounting for the spectral response functions of the space sensor S^s;

$\Re^i$: modeled *in situ* hyperspectral values determined from $\Re^r$ accounting for the spectral response functions of the in situ sensor S^i defined using Gaussian functions, and varying the bandwidth and center-wavelength of the hypothetical *in situ* instrument;

$\Re^{r'}$: reconstructed L_W and E_S spectra at 0.1 nm resolution using $\Re^i$;

$\Re^{s'}$: satellite-equivalent radiometric values determined from $\Re^{r'}$ (i.e., from hyperspectral data generated using simulated *in situ* reduced resolution spectra).

Briefly, with reference to the dark-gray path in Fig. 3, satellite-exact $R_{RS}^s(k)$ spectra are computed for each spectral band *k* by relying on sub-nanometer (i.e., 0.1 nm resolution) $\Re^r$ spectra (i.e., L_W^r and E_S^r). In particular, $L_W^s(k)$ and $E_S^s(k)$ data required to compute $R_{RS}^s(k)$ are determined through spectral convolution from:

$$\Re(k) = \frac{\sum_l \Re(l) S(k,l)}{\sum_l S(k,l)} \tag{1}$$

where the generic variable $\Re$ indicates $\Re^r$ and S designates the relative spectral response functions S^s of the satellite sensor, with *l* wavelength index for the 0.1 nm increment.

As opposed to $R_{RS}^s(k)$, the determination of $R_{RS}^{s'}(k)$ requires multiple steps. In agreement with the process illustrated by the light-gray path in Fig. 3, first $\Re^r$ spectra are applied to model *in situ* measurements at different spectral resolution $\Re^i$ (i.e., L_W^i and E_S^i) as acquired from ideal hyperspectral radiometers exhibiting Gaussian spectral response functions S^i at spectral bands k^i. This step is again performed through Eq. (1) where the generic variable $\Re$ indicates $\Re^r$ and S designates the relative spectral response functions S^i of the *in situ* sensor. The derived $\Re^i$ spectra are then deconvolved to reconstruct the $\Re^{r'}$ spectra at 0.1 nm through:

$$\Re^{r'}(l) = \frac{\sum_{k^i} \Re^i(k^i) S^i(k^i,l)}{\sum_{k^i} S^i(k^i,l)}, \tag{2}$$

Optics EXPRESS

where S^i is the relative spectral response function of each band k^i of the *in situ* sensor.

The derived $L_W^{r'}$ and $E_S^{r'}$ are finally convolved with the spectral response functions of the satellite sensor S^s to determine the satellite-equivalent $\Re^{s'}(k)$ (i.e., $L_W^{s'}$ and $E_S^{s'}$) required to compute $R_{RS}^{s'}(k)$. Specifically, this last convolution is also performed applying Eq. (1) with the generic variables $\Re$ indicating $\Re^{r'}$ (i.e., $L_W^{r'}$ and $E_S^{r'}$) and S designating the relative spectral response functions S^s of the satellite sensor for each spectral band *k*.

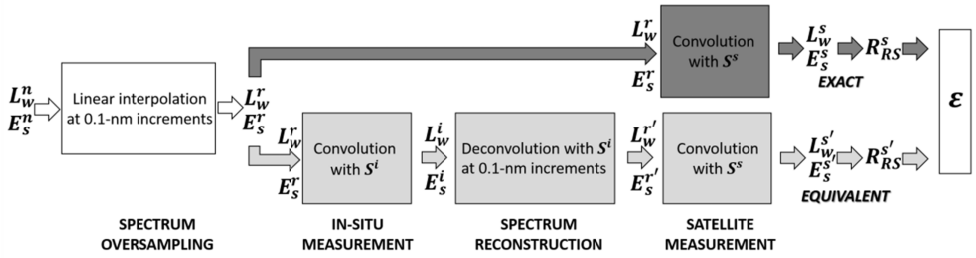

Fig. 3. Flow diagram illustrating the hyperspectral matching scheme. The comparison of satellite-equivalent $R_{RS}^{s'}$ and satellite-exact R_{RS}^{s} values is indicated by ε. See text for a comprehensive description of variables and flow.

3. Results

The comparison of satellite-equivalent $R_{RS}^{s'}$ with respect to the satellite-exact R_{RS}^{s} values are presented for each band *k* through the percent difference ε:

$$\epsilon(k) = 100\left[\frac{\Im(k) - \Im_r(k)}{\Im_r(k)}\right] \tag{3}$$

where $\Im$ indicates $R_{RS}^{s'}$ and $\Im_r$ the reference quantity R_{RS}^{s}.

Table 2 summarizes the various spectral resolution and sampling intervals considered in the analyses for the *in situ* sensor. Most of these configurations mimic spectral features of existing commercial spectrometers.

Results determined for OLCI bands displayed in Fig. 4, indicate values of ε increasing with bandwidth, $\Delta\lambda_B$, and sampling interval, $\Delta\lambda_C$, of the *in situ* sensor. When considering R_{RS} spectra from oligotrophic waters, the values of ε determined with $\Delta\lambda_B$ = 9 nm and $\Delta\lambda_C$ = 3 nm exceed 4% at 510 nm for NP and 10% at 673 nm for WM. These latter high values are explained by spectral features located in the vicinity of the specific center-wavelength (note that these differences correspond to very low absolute values of R_{RS} of the order of 10^{-5} sr^{-1}). Still, in the most favorable case given by $\Delta\lambda_B$ = 1 nm and $\Delta\lambda_C$ = 1 nm, ε does not generally exceed ±0.1%.

Optics EXPRESS

Table 2. Spectral resolutions $\Delta\lambda_B$ and sampling intervals $\Delta\lambda_C$ considered for the application of the hyperspectral matching scheme.

ΔλB [nm]	ΔλC [nm]	Comments
1	1	Comparable to MOS
2	2	
3	1	
6	2	
9	3	Comparable to RAMSES

In contrast to oligotrophic waters, R_{RS} representing optically complex cases generally exhibit values of ε within ±1% regardless of $\Delta\lambda_B$ and $\Delta\lambda_C$.

Because of the higher resolution of the satellite sensor bands, the same analysis performed for PACE-like bands exhibits larger values of ε than those determined for OLCI in the spectral regions with large changes in the slope of R_{RS} . Specifically, in Fig. 5 the ε values determined with $\Delta\lambda_B$ = 9 nm and $\Delta\lambda_C$ = 3 nm exceed 4% for oligotrophic waters (e.g., at around 515 nm for NP, and, near 605 nm and 665 nm for both NP and WM). With $\Delta\lambda_B$ = 2 nm and $\Delta\lambda_C$ = 2 nm the value of ε is generally within ±0.5% in oligotrophic waters and within ±0.1% in optically complex waters.

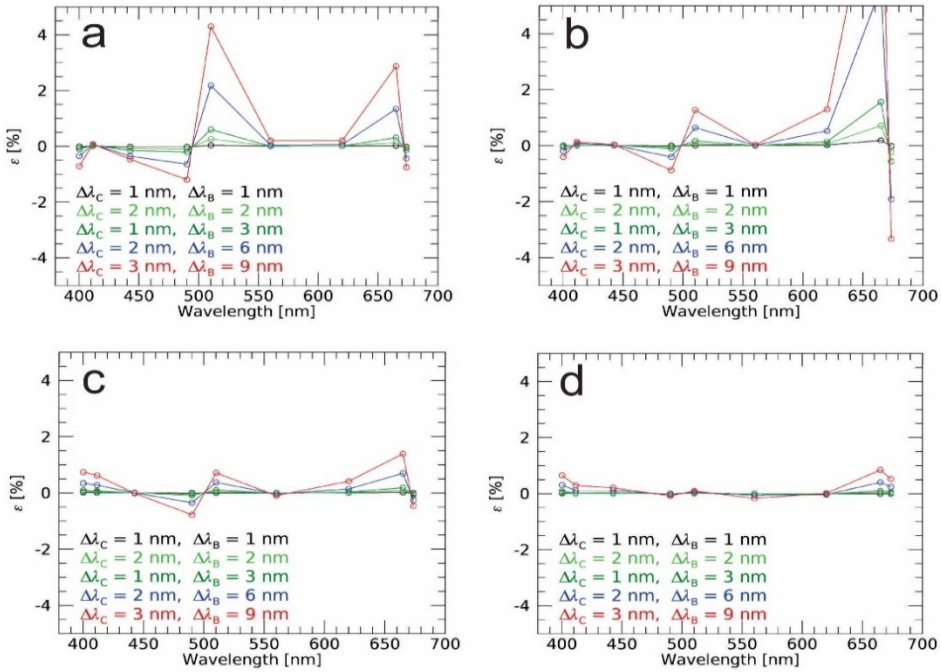

Fig. 4. Percent differences ε between $R_{rs}^{s'}$ and R_{rs}^{s} determined for OLCI bands. Data in different panels refer to the NP (a), WM (b), WB (c) and NA (d) spectra, and are presented at the OLCI center-wavelengths for different bandwidths $\Delta\lambda_B$ and spectral sampling intervals $\Delta\lambda_C$ of the *in situ* hyperspectral sensor.

Optics EXPRESS

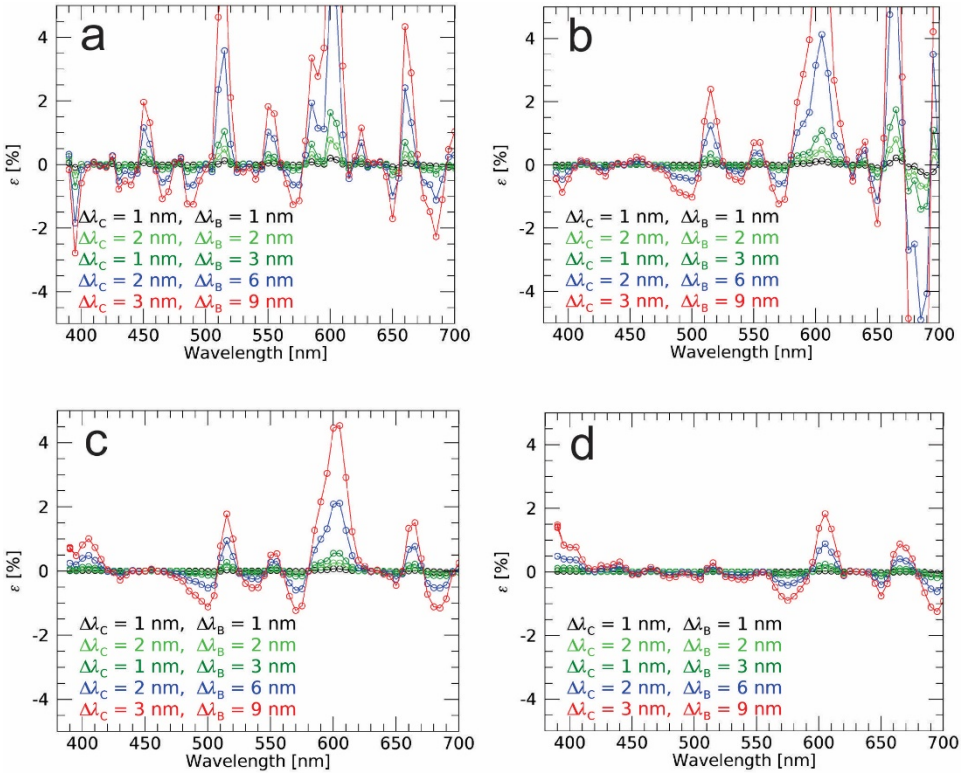

Fig. 5. Percent differences ε between $R_{RS}^{s'}$ and R_{RS}^{s} determined for PACE-like bands. Data in different panels refer to NP (a), WM (b), WB (c) and NA (d) spectra, and are presented at the considered PACE-like center-wavelengths for different bandwidths $\Delta\lambda_B$ and spectral sampling intervals $\Delta\lambda_C$ of the *in situ* hyperspectral sensor.

4. Discussion

The discussion will show how representative the hyperspectral R_{RS} for NP is for that site, the alternative use of L_w instead of R_{RS} for SVC, the uncertainties associated with values of ε determined using RAMSES R_{RS} spectra, and finally the relevance of spectral sampling intervals versus spectral resolution. Accounting for the results from the analyses presented in the previous section and of findings from the discussion topics included in this section, spectral resolution and sampling interval requirements for *in situ* hyperspectral data supporting satellite ocean color validation and SVC applications are summarized assuming strict uncertainty thresholds.

4.1 Stability of R_{RS} for the NP site

This study relies on a few hyperspectral R_{RS} spectra representative of various water types. While it is impossible in one study to include every different water type, it is still expected that these results are useful in outlining the general spectral resolution requirements for *in situ* R_{RS} supporting SVC and validation activities.

Since the NP site has been used extensively for SVC [14], it is important to consider how well the specific hyperspectral R_{RS} spectrum used in this analysis represents the MOBY site. This has been addressed with a statistically significant number (i.e., 103) of MOS spectra collected from 15 May to 28 August 2015 using the same *in situ* sensor applied for producing the spectrum included in this analysis. Using the one spectrum for the NP case is fully

supported by the mean μ and standard deviation σ of the ε values displayed in Fig. 6. Specifically, the values of ε shown in Fig. 5(a) appear equivalent to the mean values $\mu(\varepsilon)$ displayed in Fig. 6 for the 103 independent spectra from the same site. Additionally, the related standard deviations $\sigma(\varepsilon)$ exhibit values that, excluding the spectral region nearby 600 nm, do not exceed 0.4% regardless of the spectral resolution considered for the determination of ε.

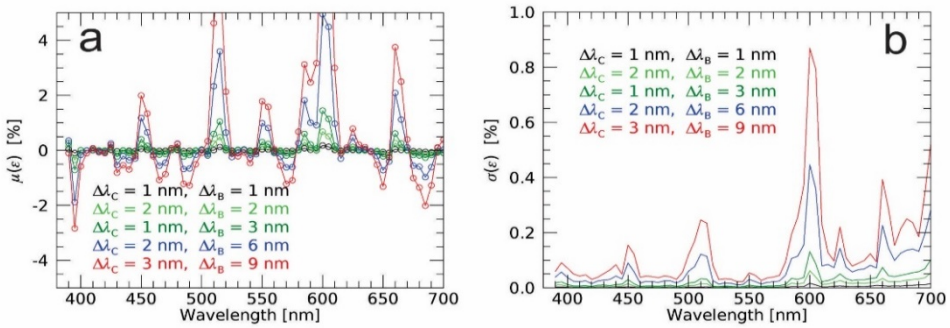

Fig. 6. Mean μ (a) and standard deviation σ (b) values of percent differences ε between $R_{RS}^{s'}$ and R_{RS}^{s} determined for PACE-like bands, and computed with 103 MOS spectra from 15 May to 28 August 2015. Data are presented at the considered PACE-like center-wavelengths for different bandwidths $\Delta\lambda_B$ and spectral sampling intervals $\Delta\lambda_C$ of the *in situ* hyperspectral sensor.

4.2 Accuracy of ε values

The relatively low spectral resolution of RAMSES data for WB, NA, and WM may lead to a misestimate of ε in spectral regions characterized by significant nanometer scaled features. This underestimate has been evaluated with the NP data, which benefit from a higher spectral resolution with respect to the other cases and additionally exhibit more pronounced spectral gradients providing added challenging conditions.

For this analysis, the MOS L_W and E_S data linearly resampled at 0.1 nm were degraded using Eq. (1) to match the RAMSES spectral resolution (i.e., $\Delta\lambda_B$ = 9 nm and $\Delta\lambda_C$ = 3 nm). Then, in agreement with the scheme outlined in Fig. 3, both full resolution and degraded MOS data were applied to calculate $R_{RS}^{s'}$ spectra. The values of ε displayed in Fig. 7 identify the spectral regions for which R_{RS} from the NP site is most affected by a reduction of spectral resolution (e.g., see regions near 385 nm, 510 nm, 600 nm and 660 nm in Fig. 7(b), which exhibit values of ε larger than ±2% for $\Delta\lambda_B$ = 9 nm and $\Delta\lambda_C$ = 3 nm).

The difference $\Delta\varepsilon$ between ε generated with Eq. (3) using the R_{RS} data that went through the RAMSES spectral response and those obtained without spectral degradation, are displayed in Fig. 8. In particular, Fig. 8(a) shows that in the case of OLCI the most pronounced misestimates of ε as a function of spectral resolution and sampling interval are observed at the 510 nm band, with differences that may reach -0.6%. These differences are explained by the high gradient in seawater reflectance near this wavelength. In summary, in the case of OLCI bands it can be assumed that 0.6% is a tentative estimate of the maximum uncertainty that would affect the previous analysis performed with R_{RS} data from NP, if collected with a spectral resolution of 9 nm and sampling interval of 3 nm (i.e., close to the spectral features of RAMSES data).

In the case of PACE-like bands, the values of $\Delta\varepsilon$ in Fig. 8(b) exceed ±1% near a few center-wavelengths (i.e., 510 nm, 600 nm, 660 nm and, with some caution, 495 nm) for the lowest spectral resolution and sampling interval (i.e., 9 nm and 3 nm, respectively).

Overall, the previous results confirm misestimates of ε for the analyses performed with RAMSES spectra. It is expected, however, that for optically complex waters (i.e., NA and WB), misestimates will be lower than those quantified through R_{RS} from NP due to R_{RS} naturally exhibiting less pronounced spectral features in these other locations. Thus, it can be assumed that results from the analyses of RAMSES spectra can be applied with some confidence to draw general conclusions in optically complex waters, even though it probably leads to an underestimate of requirements. Nevertheless, the case of the WM oligotrophic waters is more affected by the reduced spectral resolution of RAMSES sensors and these results should only be considered in combination with those determined from R_{RS} related to NP.

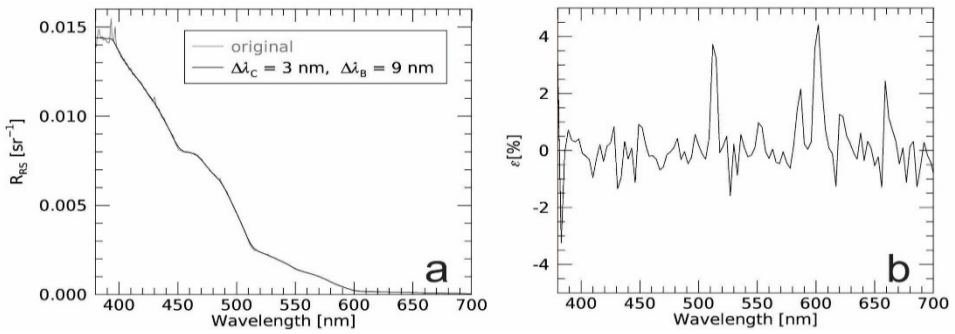

Fig. 7. Original (grey line) and spectrally degraded NP R_{RS} data (black line) determined with $\Delta\lambda_C$ = 3 nm and $\Delta\lambda_B$ = 9 nm (a), and percent differences ε between degraded and the original high resolution spectra (b).

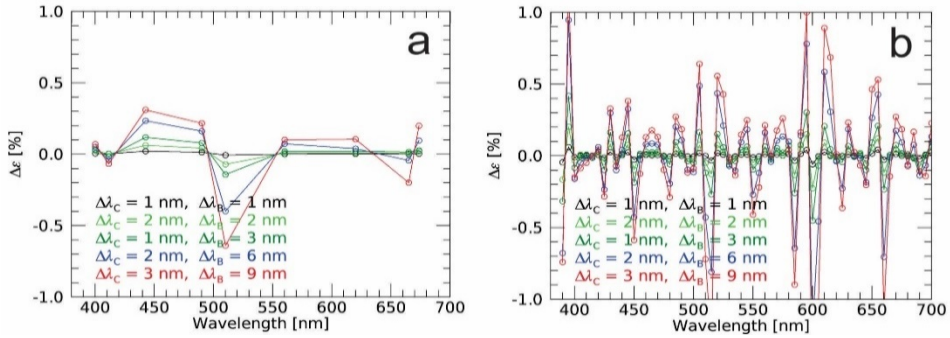

Fig. 8. Differences $\Delta\varepsilon$ between values of ε determined from $R_{RS}^{s'}$ and R_{RS}^{s} for the OLCI (a) or PACE-like (b) bands, with reduced resolution (i.e., $\Delta\lambda_B$ = 9 nm and $\Delta\lambda_C$ = 3 nm) and full resolution NP spectra.

It is emphasized that the relatively low impact of spectral degradation resulting from the previous analysis is largely explained by the "smoothness" of the R_{RS} spectrum obtained through the normalization of L_W to E_S. In fact, this process removes the high spectral resolution features due to the solar spectrum and atmospheric absorption that affect L_W. Consequently, the same conclusions achieved for R_{RS} do not likely apply to RAMSES L_W spectra.

4.3 L_W versus R_{RS}

The overall analysis has been based on R_{RS} data that are the target quantity for most ocean color applications. However, SVC is often performed using L_W data [14,15]. This alternative solution avoids dealing with uncertainties of computed or measured downward irradiance E_S,

but increases the spectral resolution requirements for *in situ* radiometry due to the higher spectral complexity of the L_W compared with the R_{RS} spectra. This is shown in Fig. 9 by the percent differences ε computed using Eq. (3) with $\mathfrak{z}$ indicating $L_W^{s'}$ and $\mathfrak{z}_r$ the reference quantity L_W^s from NP spectra (the same analysis is not presented for RAMSES data due to their relatively low spectral resolution). These ε values, when compared to those displayed in Fig. 4(a), do not show a significant impact of the use of L_W or R_{RS} on spectral resolution requirements for multispectral satellite sensors such as OLCI when excluding the bands in the blue spectral region. Similarly, the values of ε determined for the PACE-like bands exhibit a marked increase in the blue spectral region near 395 nm, 400 nm and 430 nm, when compared to those shown in Fig. 5(a). This is fully explained by the pronounced spectral features of L_W in the blue spectral region. The comparison of Fig. 10 with Fig. 7, which display full resolution and spectrally degraded data for both L_W and R_{RS} together with the related values of ε, shows the higher spectral complexity of L_W and the importance of using higher resolutions *in situ* sensors for applications requiring L_W with respect to R_{RS} .

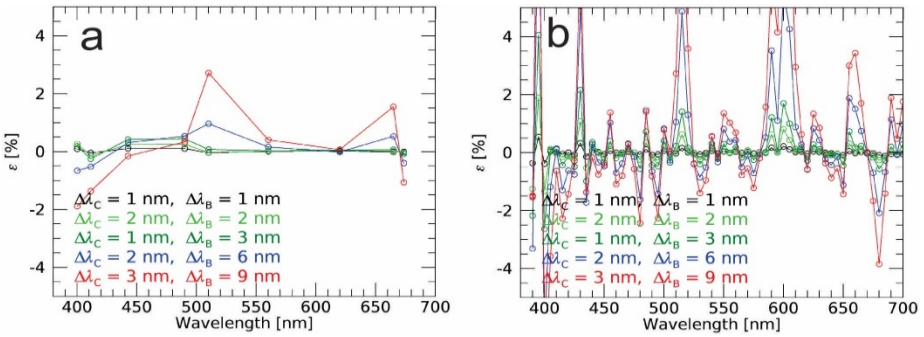

Fig. 9. Percent differences ε between $L_w^{s'}$ and L_w^s determined with NP spectra for OLCI (a) or PACE-like (b) bands. Data are presented at the considered OLCI or PACE-like center-wavelengths for different simulated bandwidths $\Delta\lambda_B$ and spectral sampling intervals $\Delta\lambda_C$ of the *in situ* hyperspectral sensor.

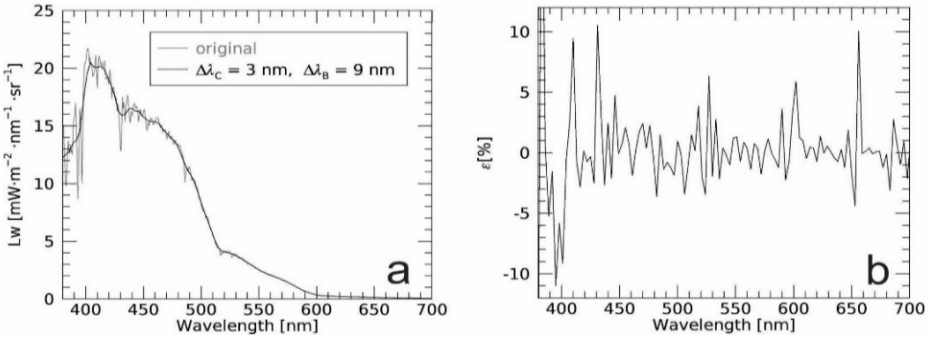

Fig. 10. Original (grey line) and spectrally degraded NP L_w data (black line) determined with $\Delta\lambda_C$ = 3 nm and $\Delta\lambda_B$ = 9 nm (a), and percent differences ε between degraded and the original high resolution spectra (b).

4.4 Spectral sampling interval versus resolution

Spectral resolutions $\Delta\lambda_B$ and sampling intervals $\Delta\lambda_C$ considered in the previous analysis are limited to a few cases guided by the specifications of existing spectrometers. When looking at results presented in Figs. 4 and 5, the configuration defined by $\Delta\lambda_B$ = 2 nm and $\Delta\lambda_C$ = 2 nm exhibits a slightly better performance than that given by $\Delta\lambda_B$ = 3 nm and $\Delta\lambda_C$ = 1 nm. This

clearly indicates the importance of spectral resolution over sampling interval in requirements for hyperspectral ocean color sensors. This is fully confirmed by the additional analysis presented in Fig. 11 and performed for the NP case by setting $\Delta\lambda_B$ = 6 nm, or alternatively $\Delta\lambda_B$ = 3 nm, with $\Delta\lambda_C$ varying from 1 nm to $\Delta\lambda_B$ in 1 nm increments. These results indicate that when $\Delta\lambda_C$ approaches or is lower than $\Delta\lambda_B$ /2, differences with respect the reference configuration defined by $\Delta\lambda_C$ = 1 nm become irrelevant (i.e., drop within ±0.01%). This implies that in agreement with Nyquist sampling theory, oversampling with $\Delta\lambda_C$ lower than approximately $\Delta\lambda_B$ /2 does not lead to any significant increase in accuracy.

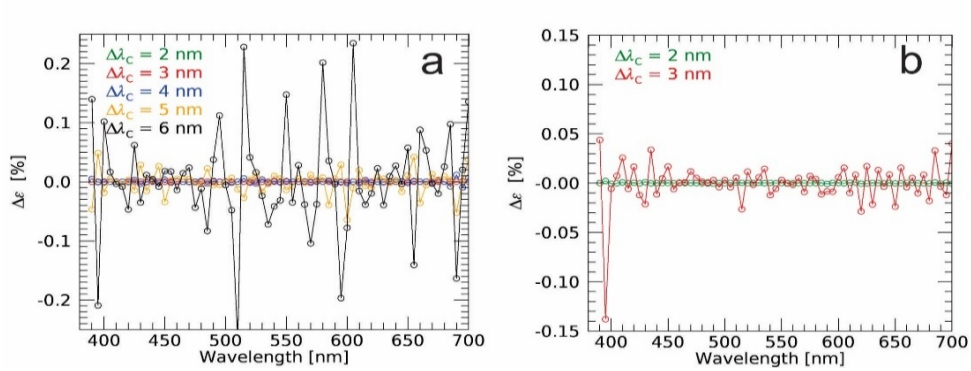

Fig. 11. Differences $\Delta\varepsilon$ between values of ε determined from $R_{rs}^{s'}$ and R_{rs}^{s} at the PACE-like bands, with reduced and full resolution (i.e., with $\Delta\lambda_C$ = 1 nm and $\Delta\lambda_B$ = 1 nm) NP spectra. Specifically, data in the various panels refer to $\Delta\varepsilon$ for various spectral degradation defined assuming fixed bandwidths (i.e., $\Delta\lambda_B$ = 6 nm (a) and $\Delta\lambda_B$ = 3 nm (b)) and different spectral sampling intervals $\Delta\lambda_C$.

4.5 Uncertainty requirements

The Implementation Plan for the Global Observing System for Climate (GCOS [1]) indicates a 5% uncertainty requirement for ocean color radiometric data products (i.e., L_W) in the blue-green spectral regions, and additionally the need for 0.5% radiometric stability per decade.

Considering that uncertainties affecting *in situ* radiometric data [9] result from a number of contributions (e.g., calibration, environmental and superstructure perturbations, and data reduction through subsurface extrapolation, self-shading, correction for bidirectional effects), it is important that the maximum difference due to spectral matching is well below the target uncertainty defined for validation and SVC. Accounting for expected uncertainty budgets of highly accurate radiometric measurements [16] and recognizing that accuracy requirements are much more demanding for SVC than for validation, strict thresholds of ε within ±1% and of ε within ±0.5% are applied in the following analysis for validation and SVC activities performed with R_{rs} , respectively. It is underlined that the small values chosen for ε are justified by the fact that perturbations introduced by spectral resolution contribute as additive terms (i.e., biases) to the uncertainty budget of each specific mission, and consequently may directly affect the 0.5% GCOS stability requirement per decade. Additionally, while some of the other contributions to the overall uncertainty budget are difficult to minimize (e.g., environmental effects), the one solely due to spectral resolution can be reduced to negligible values by instrument design.

Thus, emphasizing that the spectral matching problem is addressed from the pure radiometric point of view without considering any potential correction for the *in situ* values (e.g., band-shifting), spectral resolution requirements for both validation and SVC applications are determined from the results summarized in the previous sections. Specifically, assuming that the spectral sampling interval $\Delta\lambda_C$ is close to or lower than half the

Optics EXPRESS

spectral resolution (i.e., $\Delta\lambda_C \leq \Delta\lambda_B/2$), results from Figs. 4-5 lead to the subsequent requirements solely based on R_{RS} data.

For SVC activities, which are commonly performed in oligotrophic waters [15] and consequently by solely considering findings from the analysis of R_{RS} from ultra-oligotrophic waters, the following general conclusions can be drawn with ε within ±0.5% in the blue-green spectral region:

- A spectral resolution better than 3 nm is required for *in situ* hyperspectral sensors in the case of satellite multispectral sensors (as shown for OLCI bands in Fig. 4(a));
- Conversely, a spectral resolution better than 1 nm is recommended for *in situ* sensors in the case of satellite hyperspectral sensors (as shown for PACE-like bands in Fig. 5(a)). The previous requirement can be relaxed to 2 nm when excluding spectral regions near 510 nm, 600 nm and, with caution, at 395 nm.

For validation activities performed with R_{RS} setting ε within ±1% in the blue-green spectral region:

- The spectral resolution of *in situ* hyperspectral sensors should be better than 3 nm in oligotrophic waters in the case of satellite multispectral sensors. The requirements can be relaxed to a spectral resolution better than approximately 9 nm for optically complex waters (as shown for OLCI bands in Fig. 4).
- The spectral resolution of *in situ* hyperspectral sensors should also be better than 3 nm in oligotrophic waters in the alternative case of satellite hyperspectral sensors. Excluding bands near 600 nm, spectral resolution better than 6 nm may satisfy requirements for optically complex waters (as shown for PACE-like bands in Fig. 5).

It is important to remember, however, that the previous spectral resolution requirements defined for optically complex waters may be somewhat underestimated having been determined using *in situ* hyperspectral data with relatively low spectral resolution. Obviously, a different target ε would imply more or less stringent requirements. Additionally, the use of L_W instead of R_{RS}, would increase requirements ultimately indicating the need for sub-nanometer resolution in the blue spectral region for hyperspectral sensors such as PACE.

5. Summary and conclusions

An estimate of the uncertainties (actually biases) affecting comparisons of *in situ* and satellite radiometric matchups has been derived as a function of spectral band characteristics of *in situ* sensors. This analysis, that has relevance for SVC applications and satellite ocean color validation relying on the use of *in situ* R_{RS} data, has been developed using *in situ* hyperspectral radiometric data representative of different water types: oligotrophic and optically complex. These spectra have been used to construct hyperspectral data characterized by different spectral resolution and sampling intervals, successively applied to quantify differences between *in situ* and satellite R_{RS} values.

Results obtained for the OLCI visible bands, indicate that differences may reach several percent in oligotrophic waters with spectral resolution and sampling intervals of 9 nm and 3 nm, respectively. Considering the same resolution and sampling interval, differences are always within ±1% in optically complex waters.

In the case of PACE-like visible bands defined by 5 nm width, Gaussian spectral response and 5 nm sampling interval, differences may also exhibit values exceeding several percent as a function of the water type and spectral resolution of the *in situ* sensor.

Optics EXPRESS

The analysis has also shown that the sampling interval of the *in situ* hyperspectral sensors should be close to half the spectral resolution and that, in agreement with the Nyquist sampling theory, any oversampling does not provide significant benefits.

An attempt to define requirements for the spectral resolution of *in situ* hyperspectral radiometers supporting validation and SVC applications through R_{RS} spectra led to diverse requirements. Setting the target difference to ±1% in the blue-green spectral region for this one factor, validation activities in oligotrophic waters require spectral resolutions better than 3 nm for both OLCI and PACE-like bands. Spectral resolution requirements in optically complex waters, which are likely underestimated, result in values of 6 nm for PACE-like bands and 9 nm for OLCI.

SVC applications, restricted to oligotrophic waters, imply a higher accuracy when compared to validation activities. Assuming a maximum difference of ±0.5% between *in situ* and satellite R_{RS} data in the blue-green spectral region, the analysis performed for OLCI indicates the need for hyperspectral *in situ* data to be collected with a spectral resolution better than 3 nm. In the case of PACE, the spectral resolution needs to be lower than 1 nm, or alternatively 2 nm when excluding spectral regions nearby 510 nm, 600 nm and likely 395 nm.

When using L_W instead of R_{RS}, the study also indicates more stringent requirements for *in situ* hyperspectral data due to the added spectral features of the incident solar irradiance spectrum and atmospheric absorption, which are minimized in R_{RS} by the normalization of L_W with respect to the downward irradiance E_S.

These stringent requirements on spectral resolution of *in situ* hyperspectral sensors result from the adoption of strict uncertainty requirements for satellite radiometric products. Thus it is recognized that a relaxation of spectral resolution requirements is feasible for non-critical applications of *in situ* data such as validation activities performed in challenging measurement conditions (e.g., high spatial inhomogeneity of seawater optical properties, low sun elevations, non-oceanic aerosols), where other factors dominate the quality of the matchup analysis.

Funding

Joint Research Centre (JRC); National Oceanic and Atmospheric Administration (NOAA) (NA15OAR4320064, NOAA2012-09-0004); National Aeronautics and Space Administration (NASA) (NNX14AP63G).

Acknowledgments

The authors would like to thank Stephanie Flora for providing the MOS data essential for the analysis presented in the work and additionally some of the data presented in Table 1.

Certain commercial instruments and suppliers are identified in this paper to foster understanding. Such identification does not imply recommendation or endorsement by any of the Institutions involved in the study, nor does it imply that the equipment identified is necessarily the best available for the purpose.